Ribosome-induced changes in elongation factor Tu conformation control GTP hydrolysis

Elizabeth Villa[a,b,1], Jayati Sengupta[c,1,2], Leonardo G. Trabuco[a,b], Jamie LeBarron[c], William T. Baxter[c], Tanvir R. Shaikh[c], Robert A. Grassucci[d], Poul Nissen[e], Måns Ehrenberg[f], Klaus Schulten[a,g], and Joachim Frank[d,h,3]

[a]Beckman Institute, University of Illinois at Urbana-Champaign, Urbana, IL 61801; [b]Center for Biophysics and Computational Biology, University of Illinois at Urbana-Champaign, Urbana, IL 61801; [c]Wadsworth Center, Empire State Plaza, Albany, NY 12201; [d]Howard Hughes Medical Institute, Department of Biochemistry and Molecular Biophysics, Columbia University, 650 West 168th Street, New York, NY 10032; [e]Department of Molecular Biology, University of Aarhus, Gustav Wieds vej 10C, DK-8000 Aarhus, Denmark; [f]Department of Cell and Molecular Biology, Biomedical Center, Box 596, S-75124 Uppsala, Sweden; [g]Department of Physics, University of Illinois at Urbana-Champaign, Urbana, IL 61801; and [h]Department of Biological Sciences, Columbia University, 600 Fairchild Center, Mail Code 2402, 1212 Amsterdam Avenue, New York, NY 10027

Contributed by Joachim Frank, November 12, 2008 (sent for review October 10, 2008)

In translation, elongation factor Tu (EF-Tu) molecules deliver aminoacyl-tRNAs to the mRNA-programmed ribosome. The GTPase activity of EF-Tu is triggered by ribosome-induced conformational changes of the factor that play a pivotal role in the selection of the cognate aminoacyl-tRNAs. We present a 6.7-Å cryo-electron microscopy map of the aminoacyl-tRNA·EF-Tu·GDP·kirromycin-bound *Escherichia coli* ribosome, together with an atomic model of the complex obtained through molecular dynamics flexible fitting. The model reveals the conformational changes in the conserved GTPase switch regions of EF-Tu that trigger hydrolysis of GTP, along with key interactions, including those between the sarcin-ricin loop and the P loop of EF-Tu, and between the effector loop of EF-Tu and a conserved region of the 16S rRNA. Our data suggest that GTP hydrolysis on EF-Tu is controlled through a hydrophobic gate mechanism.

decoding | GTPase | flexible fitting | cryo-EM | ternary complex

In the elongation cycle of protein synthesis, each aminoacyl-tRNA (aa-tRNA) is delivered to the mRNA-programmed ribosome as a ternary complex with elongation factor Tu (EF-Tu) and GTP. On binding to the ribosome, aa-tRNA enters the A/T state, where it occupies the A site on the 30S ribosomal subunit while still interacting with EF-Tu. When the codon–anticodon interaction is cognate, GTPase activity of EF-Tu is greatly stimulated and GTP hydrolysis occurs rapidly, inducing a large conformational change of EF-Tu followed by its dissociation from the ribosome and subsequent accommodation of aa-tRNA into the ribosomal A site. The irreversible GTP hydrolysis separates 2 kinetic steps of aa-tRNA incorporation, namely initial selection and proofreading, that jointly establish the overall accuracy of tRNA selection by the codon-programmed ribosome (1). Much effort has been devoted to elucidate the mechanism by which codon recognition in the 30S subunit leads to GTP hydrolysis by EF-Tu >75 Å away. Biochemical and structural studies identified some key interactions, but the atomic details of the mechanism have remained elusive. In particular, the transduction of the codon recognition signal and subsequent ribosome-induced EF-Tu conformational changes leading to GTPase activation are not well understood.

GTP hydrolysis in EF-Tu takes place through an in-line, direct attack on the γ-phosphate by a water molecule (2). His-84 of EF-Tu has been proposed to activate a water molecule for nucleophilic attack on the γ-phosphate by extracting one of its protons (3, 4). This proposal agrees with studies identifying His-84 as the catalytic residue that stabilizes the transition state of GTP hydrolysis by hydrogen bonding to the attacking water molecule or the γ-phosphate group of GTP (5). Crystal structures of EF-Tu in the GTP form revealed a "hydrophobic gate" that appears to control access of His-84 to the GTP binding pocket (3, 6). For His-84 to carry out its catalytic role and activate the water molecule, the gate would have to open on interaction with the ribosome (3, 6). So far, gate opening has only been observed in the crystallographic structure of *Thermus thermophilus* EF-Tu in complex with GDP and the GTPase-stimulating antibiotic methyl-kirromycin (aurodox), outside the ribosome.

In the present work, we focus on the ribosome-induced EF-Tu conformational changes that trigger GTP hydrolysis on the factor as revealed by cryo-electron microscopy (cryo-EM) studies. We provide structural evidence suggesting that the ribosome induces the opening of the hydrophobic gate and the repositioning of His-84 of EF-Tu. Our results reconcile a large body of experimental data and explain how the ribosome controls the GTPase activity of EF-Tu in the ternary complex.

Results

We obtained a 6.7-Å cryo-EM map of the preaccommodated *Escherichia coli* 70S ribosome bound to the Phe-tRNA^{Phe}·EF-Tu·GDP ternary complex stalled by the antibiotic kirromycin (kir) (7). We applied the recently developed molecular dynamics flexible fitting (MDFF) method (8) to obtain an atomic model of the complex that enables the interpretation of the cryo-EM data in unprecedented detail. The map, along with the fitted atomic model of the 70S ribosome, the ternary complex, P- and E-site tRNAs, and mRNA are shown in Fig. 1*A*. This map presents a substantial advancement in resolution over previously reported cryo-EM data (9–11), allowing us to corroborate previous observations in greater detail, and to observe new contacts and changes in conformation of the complex. In particular, with the improvement in resolution, the structural features of EF-Tu and its interactions with the ribosome are clearly discernible in the density map.

The relative orientation between the domains of the ribosome-bound EF-Tu with kirromycin (Fig. 1*B*) is most similar to

Author contributions: M.E., K.S., and J.F. designed research; E.V., J.S., L.G.T., J.L., W.T.B., T.R.S., and R.A.G. performed research; M.E. contributed new reagents/analytic tools; E.V., J.S., L.G.T., J.L., W.T.B., T.R.S., P.N., and K.S. analyzed data; and E.V., J.S., L.G.T, K.S., P.N., and J.F. wrote the paper.

The authors declare no conflict of interest.

Freely available online through the PNAS open access option.

Data deposition. The atomic coordinates have been deposited in the Protein Data Bank, www.pdb.org [PDB ID codes 3FIH (30S and factors) and 3FIK (50S)]. The cryo-EM density map has been deposited in the 3D-EM database, EMBL-European Bioinformation Institute (code EMD-5036).

See Commentary on page 969.

[1]E.V. and J.S. contributed equally to this work.

[2]Present address: Structural Biology and Bioinformatics Division, Indian Institute of Chemical Biology, Calcutta, 700032, India.

[3]To whom correspondence should be addressed. E-mail: jf2192@columbia.edu.

This article contains supporting information online at www.pnas.org/cgi/content/full/0811370106/DCSupplemental.

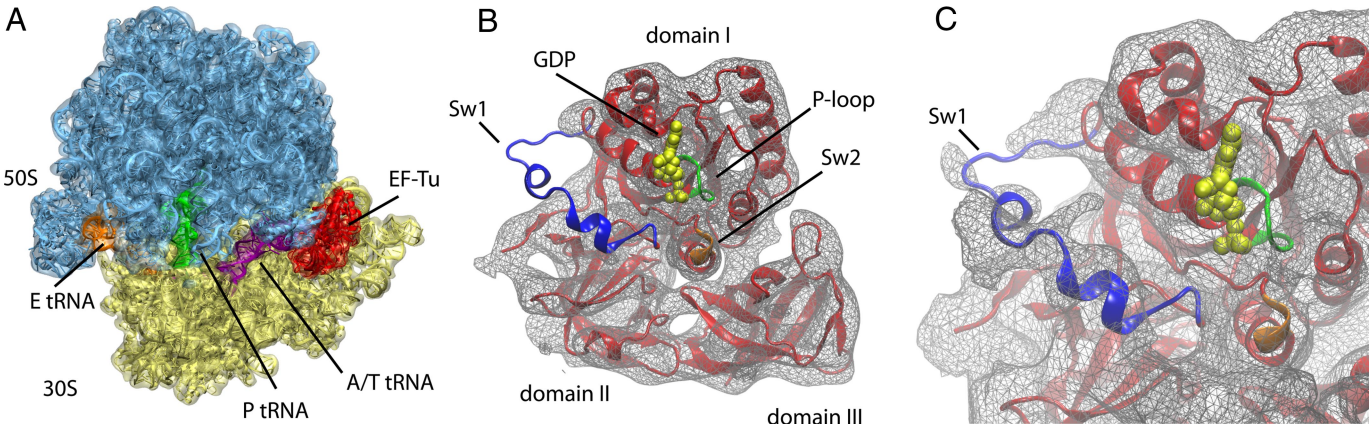

Fig. 1. Overview of EF-Tu structure bound to the ribosome. (*A*) Cryo-EM map of the 70S·fMet-tRNA^{fMet}·Phe-tRNA^{Phe}·EF-Tu·GDP·kir complex at a resolution of 6.7 Å shown in transparent surface. The atomic model obtained by molecular dynamics flexible fitting (MDFF) is shown in cartoon representation. (*B*) Atomic model of the ribosome-bound EF-Tu showing a domain orientation most similar to the closed, GTP-bound form. The switch regions are highlighted: switch I (Sw1) in blue, switch II (Sw2) in orange, and P-loop in green. The same coloring scheme is used in all figures. (*C*) Closeup of the GTPase domain of EF-Tu. The cryo-EM density map is displayed at a lower threshold to make the switch I density visible. Density thresholds are 2.6 σ (*A*), 2.2 σ (*B*), and 1.4 σ (*C*).

the "closed," GTP-bound form of EF-Tu (3, 6), as previously observed outside of the ribosome. The structure of EF-Tu·GDP·kir bound to the ribosome has been proposed to correspond to a state immediately after GTP hydrolysis, yet preceding the conformational change into the free, GDP-bound structure and, hence, preceding EF-Tu release (11). Our data show that this EF-Tu structure indeed corresponds to an activated state for the hydrolysis of the nucleotide, as detailed below. Several conserved regions playing prominent roles in the working cycle of GTPases, namely switch I (EF-Tu residues 40–62; *E. coli* numbering is used throughout this article), switch II (80–100) and P loop (18–23), are found to undergo characteristic conformational changes in EF-Tu. We describe these changes in the context of the ribosome-bound state of EF-Tu captured by the map.

GTPase Activation Is Controlled by a Hydrophobic Gate. The hydrophobic gate of EF-Tu, represented schematically in Fig. 2*A*, is formed by residues Val-20 (P loop) and Ile-60 (switch I). The gate in its closed form is present in many crystal structures of GDP- and GTP-bound EF-Tu both bound and unbound to tRNA, indicating that gate opening occurs only in the presence of the ribosome. Fig. 2*B* shows the hydrophobic gate present in the crystal structure of the free *E. coli* ternary complex (PDB ID code 1OB2; unpublished data). The aurodox-bound structure, shown in Fig. 2*D*, displays an open gate, where Ile-60 and the remainder of switch I are disordered and His-84 is repositioned toward the nucleotide (12), hinting that the increased GTPase activity induced by aurodox is achieved by gate opening. One wing of the hydrophobic gate is formed by residue Val-20, which forms part of the P loop, a conserved element in GTPases important in guanine nucleotide release (13, 14). Our structure shows that the P-loop interacts with the sarcin-ricin loop (SRL; nucleotides 2646–2674 of the 23S rRNA). It was established that SRL interacts with EF-Tu (see ref. 11 and references therein), but available cryo-EM data until now lacked the resolution needed to identify the residues of EF-Tu involved in this interaction. Fig. 3

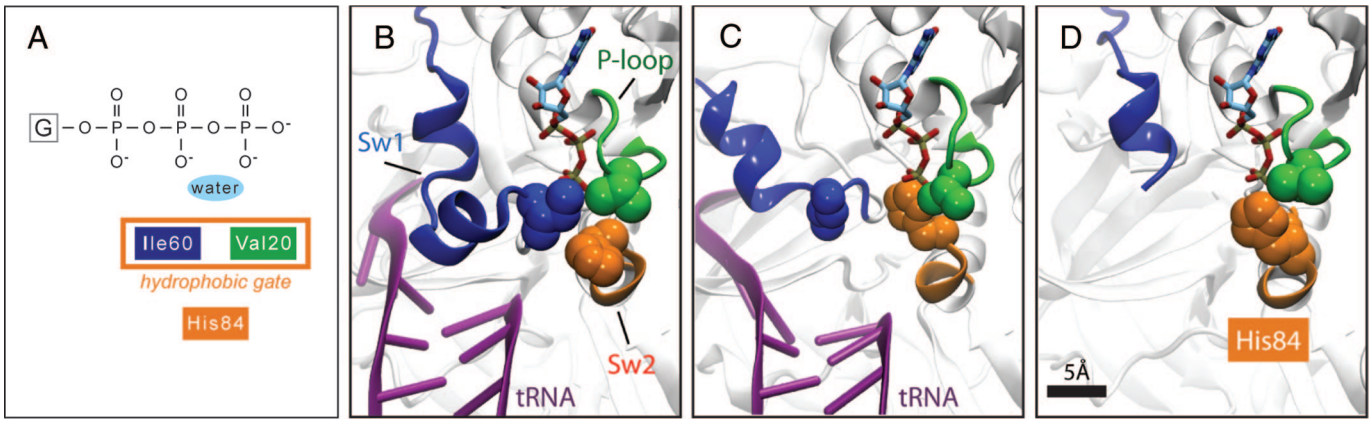

Fig. 2. Hydrophobic gate. (*A*) Schematic representation of the hydrophobic gate formed by EF-Tu residues Ile-60 and Val-20, which prevents His-84 from activating the water molecule and thus catalyzing GTP hydrolysis (G, guanisine). (*B*) The gate shown in the crystal structure of the ternary complex bound to kirromycin (PDB ID code 1OB2; unpublished data). (*C*) The ribosome-bound ternary complex model obtained through MDFF displaying conformational changes in the nucleotide binding area. Switch I has moved away, opening the gate on the Ile-60 side; the acceptor stem of the tRNA has moved significantly closer to switch II; and the side chain of His-84 has been repositioned toward the nucleotide, resulting in catalysis of GTP hydrolysis. (*D*) Open hydrophobic gate seen in the crystal structure of the aurodox-bound EF-Tu [PDB ID code 1HA3 (12)]. The structure suggests that an opening of the hydrophobic gate is necessary for hydrolysis, and exhibits a conformation of the gate very similar to that obtained by cryo-EM and MDFF. A GTP molecule is shown in *B–D* for comparison purposes, to illustrate the spacial rearrangements in the hydrophobic gating, although the structures depicted were obtained in presence of GDPNP (*B*) and GDP (*C* and *D*). The coordinates of the GTP molecule correspond to those of GDPNP in the crystal structure depicted in *B*; the coordinates of the nucleotides present in the structures depicted in *C* and *D* are very similar.

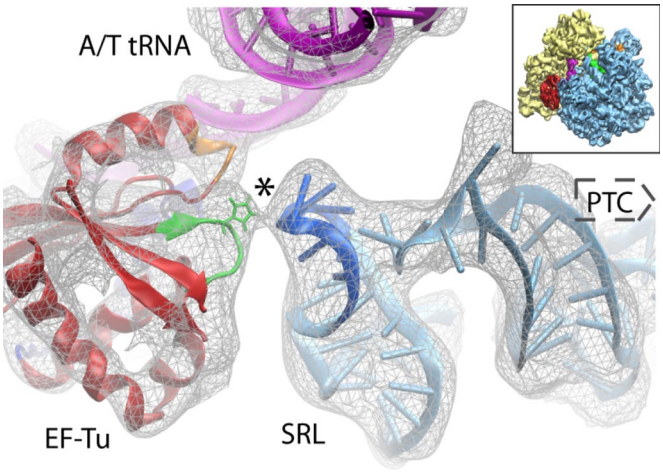

Fig. 3. Interaction (marked with an asterisk) between His-19 in the P loop of EF-Tu (green) and A2260 in the tetraloop of the SRL (cyan; tetraloop shown in blue). This interaction presumably establishes an anchor point holding one of the wings of the hydrophobic gate (compare Fig. 2) in place. (*Inset*) The ribosome is shown in the same orientation. The map is contoured at 2.5 σ. This figure is rotated 90° with respect to the view in Fig. 2.

shows the residues as resolved in our MDFF analysis, namely His-19 of EF-Tu and A2660 in the tetraloop of SRL. Because of the importance of the P loop for nucleotide exchange in EF-Tu (14), one may expect that interaction with SRL pulls the P loop away from the nucleotide binding pocket, thereby opening the gate through a mechanism similar to nucleotide exchange. However, our analysis shows that the contact with SRL stabilizes the P loop in its position, acting as an anchor point for this wing of the gate, whereas the other wing opens as described below. The P loop-SRL interaction might also be involved in signal transduction after GTP hydrolysis from the G domain of EF-Tu to the peptidyltransferase center (PTC), inducing conformational changes in the PTC required for complete accommodation and efficient peptide bond formation (see refs. 15 and 16 and references therein).

The other wing of the hydrophobic gate (Ile-60) is part of switch I (also known as effector loop), which assumes an α-helix conformation in the closed form of EF-Tu and changes to a β-hairpin conformation in the open form (17, 18). The large flexibility of this region has prevented switch I from being resolved in EM density maps and some crystallographic structures. At low-density threshold, the present map displays clear density corresponding to switch I; i.e., all molecular surfaces are solid, without disruption by spikes or other noisy features. The map allowed us to build an atomic model of switch I interacting with the ribosome (Fig. 4*A*; see *Materials and Methods*). In the state captured by the map, switch I interacts with the junction formed by helices h8 and h14 of the 16S rRNA (Fig. 4 *A* and *B*). It is interesting to note that a similar interaction was recently observed between the eukaryotic 40S subunit and the elongation factor eEF2 in a cryo-EM map of a transition-state complex (19), suggesting that this interaction is already present before GTP hydrolysis. The conformation of switch I in the ribosome-bound EF-Tu is different from that in the closed (GTP) and open (GDP) forms of free EF-Tu. The conformational change from the closed form involves repositioning of the wing containing Ile-60 leading to the opening of the hydrophobic gate, as depicted in Fig. 2*C*. This scenario receives support from the previous observation that cleavage of the peptide bond between Arg-58 and Gly-59 in switch I of EF-Tu abolishes ribosome-induced GTPase activation (20), because interruption of this peptide bond should prevent the movement of switch I from opening the hydrophobic gate. The effect of the interaction between switch I and the 16S rRNA h8/h14 junction remains to be determined, but this contact could serve as a pathway for signal transduction to and from the decoding center through helix h44 of the 16S rRNA; this helix interacts with the decoding center at one end and with the h8/h14 junction at the other (Fig. 4*C*).

At low threshold, we also observe a bulged density in the S turn motif of SRL (nucleotides 2653–2656 of the 23S rRNA, marked with an asterisk in Fig. 4*A*). The S turn motif has been shown to be critical for EF-G binding (21), and thus it is likely that this density represents an interaction between this motif and switch I that occurs before the movement of the latter toward the h8/h14 junction; the density of the bulged region indicates that only a fraction of the particles in the sample are found in this conformation.

As depicted in Fig. 2, the third effector region of EF-Tu is switch II, which contains the catalytic residue His-84 (5). On gate opening, the side chain of His-84 is free to reach the GTP binding pocket and to activate hydrolysis. Our atomic model resolves the activating conformation of His-84 (Fig. 2*C*), which is indeed similar to the one seen in the aurodox-bound structure of EF-Tu outside of the ribosome (12), shown in Fig. 2*D*. In our model, the His-84 side chain is positioned ≈4Å from the nucleotide, i.e., much closer than the ≈8Å seen in the crystal structure of the free ternary complex that exhibits the closed hydrophobic gate (PDB ID code 1OB2, unpublished data; see also ref. 22). A comparison of all of the above structures is presented in supporting information (SI) Fig. S1. Reorientation of His-84 to form the activated state is supported by mutational data showing that replacement of Gly-83 by Ala abolishes ribosome-induced GTPase activation (23), likely because any side chain bulkier than a hydrogen in position 83 prevents the reorientation of His-84 toward the GTP binding pocket (3, 6). A similar mechanism is observed in the G protein Gα_{i1}, where rotation of the catalytic residue Gln-204 to stabilize the transition state for GTP hydrolysis requires the presence of Gly at position 203 (24).

Interaction Between EF-Tu and Ribosomal Protein L12. Another element known to interact with EF-Tu is ribosomal protein L12, which binds to the G domain of EF-Tu at helix D (25) (Table S1). L12 greatly contributes to the GTPase activity of EF-Tu on the ribosome (26), which led to the speculation that L12 induces conformational rearrangements of EF-Tu, in particular, the reorientation of His-84 (26). However, this claim could not be corroborated from structural data. In our map, helix D of EF-Tu has clear density, from which we see no evidence for conformational changes of EF-Tu in the region binding to L12. It is therefore likely that L12 stabilizes the transition state complex on the ribosome, without actively inducing the required structural rearrangements of EF-Tu.

Role of tRNA in Signal Transduction. tRNA plays a central role in GTPase activation induced by codon recognition, as suggested by several mutations (1) and by the fact that an intact tRNA is required to trigger GTP hydrolysis by EF-Tu on the ribosome (27). Previous cryo-EM data showed that the elbow of tRNA interacts with the L11-binding region of the 23S rRNA, which, together with ribosomal protein L11, constitutes the GTPase-associated center (GAC) (9, 11). Cryo-EM data at lower resolution suggested that the interaction occurs at A1067 (11); this claim was supported by mutational studies of A1067 that impair EF-Tu function (28). The present map corroborates these findings, showing that the interaction is established between a flipped A1067 of the GAC and C56 in the elbow region of the tRNA (Fig. S2). Previous molecular dynamics (MD) studies showed that A1067 can exist in 2 different conformations in solution, suggesting that the flipped-out conformation might occur during aa-tRNA binding and selection (29). Ribosomal

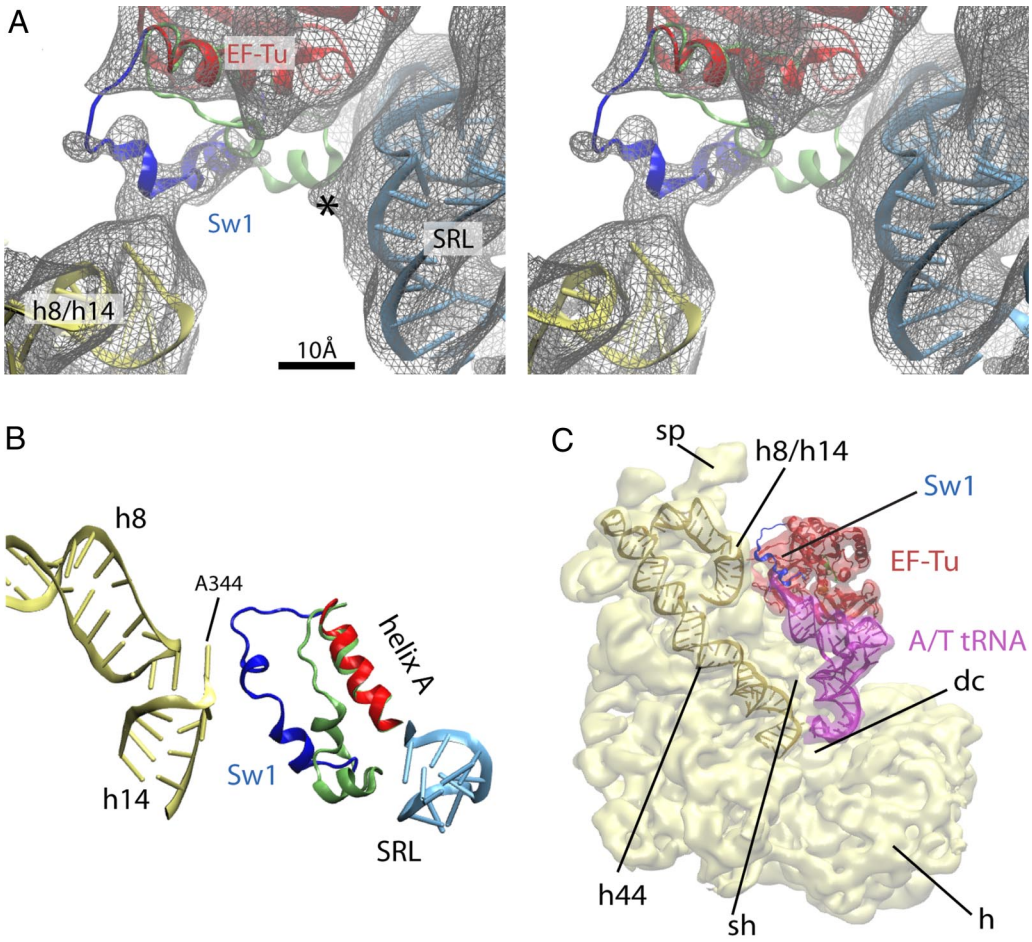

Fig. 4. Structure of switch I in the ribosome-bound EF-Tu. (*A*) Stereoview illustrating the movement of switch I (blue) toward the junction of helices h8 and h14 of 16S rRNA (yellow). Rigid-body fitting of the crystal structure (green; PDB ID code 1OB2) places switch I close to the SRL (cyan). At low-density threshold, shown as gray mesh, the density corresponding to SRL exhibits a protuberance (marked with an asterisk) around the S turn motif, possibly corresponding to an interaction with switch I (blue) during its movement toward the h8/h14 junction (yellow). The map is contoured at 1.25 σ. (*B*) Detail of the interaction between switch I and the 16S rRNA. Elements of EF-Tu (red and blue) and the 30S (yellow) and 50S (cyan) subunits are shown along with the crystal structure of switch I (green; PDB ID code 1OB2). (*C*) Overview of the ternary complex bound to the 30S subunit (yellow). switch I (blue) interacts with the h8/h14 junction; h44 interacts with the latter on one side, and with the decoding center on the other, possibly serving as part of a signal transduction pathway. Landmarks: sp, spur; sh, shoulder; dc, decoding center; h, head.

protein S12 contacts the tRNA both at the acceptor stem and the anticodon loop, connecting the movement of the acceptor stem with the reorganization of the decoding center on codon recognition (9, 10). Fig. S2 shows the residues involved in this direct link between the codon-anticodon helix and the tRNA acceptor stem through ribosomal protein S12.

Cryo-EM data had already demonstrated that the relative orientation of tRNA and EF-Tu changes on binding to the ribosome; our model reveals that even though the overall movement of tRNA is directed away from EF-Tu (Fig. S3), this rearrangement results in a closer interaction between tRNA's acceptor stem and EF-Tu's switch II, specifically with Asp-86 on switch II (Figs. 2*C*, S1, and S3). The universally conserved residue Asp-86 was proposed to play a role in stabilization of the protonated His-84 (3), and was observed to interact strongly with the tRNA in MD simulations of the free ternary complex (30). These findings, together with our structural evidence, strongly suggest that repositioning of the tRNA leading to interaction with switch II assists in the required conformational change of the latter, which results in the repositioning of His-84.

Discussion

Our data represent a significant improvement in resolution over previously reported cryo-EM structures of the ternary complex-bound ribosome. The advance toward higher resolution has allowed us to use a systematic method to obtain atomic models that explain the cryo-EM density. By using force fields that represent physical-chemical properties of biomolecules, similar to those used in X-ray crystallography structure refinement, the interpretation of the data can be pushed beyond the nominal resolution. An extensive comparison of the model obtained through the use of MDFF and models obtained through other methods is offered in ref. 8, along with a discussion of the role of resolution on the model accuracy.

Here, we presented the interactions between EF-Tu and both the ribosome and tRNA in atomic detail. The interactions induce the conformational changes necessary to trigger GTP hydrolysis on cognate codon–anticodon interaction. Our data suggest that interaction of the ternary complex with the ribosome opens a hydrophobic gate formed by residues Ile-60 and Val-20, allowing His-84 to act as a general base activating an active-site nucleophilic water molecule, and thus triggering hydrolysis.

Based on the available structural and biochemical data, we propose a refined model of aa-tRNA incorporation into the ribosome. The interaction between tRNA and GAC occurs at an early stage (11). The geometry of the codon–anticodon helix is monitored by 23S rRNA nucleotides A1492, A1493,

and G530, leading to a 30S domain closure and a tighter binding of the anticodon loop (1). This binding affects the relative orientation between tRNA and EF-Tu, a process influenced by S12. While tRNA moves, EF-Tu must be held in place, likely aided by its interaction with L12. A conformational change in switch II takes place, influenced by the acceptor stem of tRNA. Switch I of EF-Tu moves away from the nucleotide binding pocket and interacts with the junction of helices h8/h14 of the 16S rRNA, opening one wing of the hydrophobic gate, while the other wing is held fixed by the interaction between SRL and P loop. His-84 reorients toward the nucleotide, which leads to activation of a water molecule and subsequent GTP hydrolysis. After inorganic phosphate release, EF-Tu undergoes a large conformational change to an "open," GDP-bound form, leading to its dissociation from the ribosome, after which tRNA can be accommodated into the A site. The conformational change of EF-Tu can be sensed by SRL and communicated to the PTC, inducing changes in PTC required for peptide bond formation.

Materials and Methods

Cryo-EM. The sample consisted of preaccommodated *E. coli* 70S ribosome bound to the Phe-tRNA^{Phe}·EF-Tu·GDP ternary complex stalled by the antibiotic kirromycin (kir) (11) by using a standard preparation (31). The map was obtained from ≈130,000 particles, recorded with ≈58,000× magnification on a FEI Tecnai F30 Polara electron microscope operated at 300 kV at liquid-nitrogen temperature (80 K) and processed by using SPIDER. The resulting resolution of the map was estimated to be 6.7 Å with the 0.5 FCS criterion, extrapolated to the full dataset with a pixel size of 1.2 Å. A version of the map filtered to 5 Å proved to show the positions of phosphorus atoms along exposed RNA helices (7). The map represents a significant improvement in resolution over the previously published 10.3-Å map obtained from an identical sample preparation (11). The improvement in resolution was realized through optimization of image processing parameters, described in detail in ref. 7.

Flexible Fitting. The atomic model of the aminoacyl-tRNA·EF-Tu·GDP·kirromycin ternary complex-bound *E. coli* ribosome was obtained by applying the recently developed MDFF method (8). MDFF incorporates the EM data into molecular dynamics simulation as a potential proportional to the density gradient of the EM map. The potential applies forces on the atoms that actively drive the model into the density. The initial coordinates of the model were taken from available structural data. For the ribosome, an atomic model of the *E. coli* ribosome based on a 3.22-Å crystal structure (PDB ID code 2I2U/2I2V) (32) was built, as described in ref. 8. The initial structure of the ternary complex was taken from the crystal structure of *E. coli* EF-Tu in complex with kirromycin, a GTP analog, and yeast Phe-tRNA^{Phe} (PDB ID code 1OB2; unpublished data). For details on MDFF of these models to the map presented in this report, the reader is referred to ref. 8. An additional step was required to fit the structure of the switch I of EF-Tu into the density. Even though the map presents clear density corresponding to this region when visualized at low threshold, a model for switch I could not be obtained by using MDFF alone, because the gradient of the EM map in this area is not steep enough to drive the structure into the density unequivocally. Therefore, we manually fitted the helices of switch I in the GTP conformation into the density, and used the positions of the C_α atoms in this conformation as a target location for the respective atoms during MDFF simulations. The C_α atoms were driven into the target positions by introducing an additional potential term equivalent to a targeted molecular dynamics simulation (33), in which the root-mean-squared deviation between the simulated and the target positions of the C_α atoms is minimized along the simulation. In this way, the C_α atoms of switch I became located close to the target positions, whereas the rest of the atoms were still driven into the measured density, the stereochemical correctness of the model being enforced by the molecular dynamics force field.

The model produced by MDFF is useful to interpret the EM data in atomic detail; however, the atomic structure should always be analyzed together with the original data to ensure consistency and proper interpretation. Uncertainty in the coordinates arises both from features of the EM data, e.g., resolution and flexibility of certain regions, and from the conservative secondary structure restraints used in MDFF to avoid overfitting (see ref. 8 for a detailed discussion). A cryo-EM map represents an ensemble average of structures in the same functional state; certain regions can only be seen at low threshold, implying that, in the represented functional state, these regions are flexible and exist in 2 or more conformations. Combining MDFF with cryo-EM maps at resolutions like the one presented here permits the location of certain elements beyond the nominal resolution. An example is the acceptor stem of the tRNA where, even though the deviation from the crystal structure is only a few angstroms, it is clear that an overall movement of the tRNA away from the density places this regions closer to switch II of EF-Tu (Fig. S3).

All figures were made with the molecular graphics program VMD (34).

ACKNOWLEDGMENTS. We thank Andrew Carter, Zan Luthey-Schulten, and members of the Frank and Schulten labs for stimulating discussions, and Lila Iino-Rubenstein for assistance with the illustrations. This work was supported by Howard Hughes Medical Institute (J.F.), the Swedish Research Council (M.E.), National Science Foundation Grant PHY0822613 (to K.S.), and National Institutes of Health Grants P41-RR05969 (to K.S.), P41-RR01219, R37-GM29169, and R01-GM55440 (to J.F.), and R01-GM070768 (to M.E). Computer time for MDFF was supported by Large Resources Allocation Committee Grant MCA93S028 (to K.S.).

1. Ogle JM, Ramakrishnan V (2005) Structural insights into translational fidelity. *Annu Rev Biochem* 74:129–177.
2. Eccleston JF, Webb MR (1982) Characterization of the GTPase reaction of elongation factor Tu. *J Biol Chem* 257:5046–5049.
3. Kjeldgaard M, Nissen P, Thirup S, Nyborg J (1993) The crystal structure of elongation factor EF-Tu from *Thermus aquaticus* in the GTP conformation. *Structure* 1:35–50.
4. Limmer S, Reiser COA, Schirmer NK, Grillenbeck NW, Sprinzl M (1992) Nucleotide binding and GTP hydrolysis by elongation factor Tu from *Thermus thermophilus* as monitored by proton NMR. *Biochemistry* 31:2970–2977.
5. Daviter T, Wieden HJ, Rodnina MV (2003) Essential role of histidine 84 in elongation factor Tu for the chemical step of GTP hydrolysis on the ribosome. *J Mol Biol* 332:689–699.
6. Berchtold H, *et al.* (1993) Crystal structure of active elongation factor Tu reveals major domain rearrangements. *Nature* 365:126–132.
7. LeBarron J, *et al.* (2008) Exploration of parameters in cryo-EM leading to an improved density map of the *E. coli* ribosome. *J Struct Biol* 164:24–32.
8. Trabuco LG, Villa E, Mitra K, Frank J, Schulten K (2008) Flexible fitting of atomic structures into electron microscopy maps using molecular dynamics. *Structure* 16:673–683.
9. Valle M, *et al.* (2002) Cryo-EM reveals an active role for aminoacyl-tRNA in the accommodation process. *EMBO J* 21:3557–3567.
10. Stark H, *et al.* (2002) Ribosome interactions of aminoacyl-tRNA and elongation factor Tu in the codon-recognition complex. *Nat Struct Biol* 9:849–854.
11. Valle M, *et al.* (2003) Incorporation of aminoacyl-tRNA into the ribosome as seen by cryo-electron microscopy. *Nat Struct Biol* 10:899–906.
12. Vogeley L, Palm GJ, Mesters JR, Hilgenfeld R (2001) Conformational change of elongation factor Tu (EF-Tu) induced by antibiotic binding. *J Biol Chem* 276:17149–17155.
13. Vetter IR, Wittinghofer A (2001) The guanine nucleotide-binding switch in three dimensions. *Science* 294:1299–1304.
14. Dahl LD, Wieden HJ, Rodnina MV, Knudsen CR (2006) The importance of the P-loop and domain movements in EF-Tu for guanine nucleotide exchange. *J Biol Chem* 281:21139–21146.
15. Chan YL, Dresios J, Wool IG (2006) A pathway for the transmission of allosteric signals in the ribosome through a network of RNA tertiary interactions. *J Mol Biol* 355:1014–1025.
16. Blanchard SC, Gonzalez RL, Kim HD, Chu S, Puglisi JD (2004) tRNA selection and kinetic proofreading in translation. *Nat Struct Mol Biol* 11:1008–1014.
17. Abel K, Yoder MD, Hilgenfeld R, Jurnak F (1996) An α to β conformational switch in EF-Tu. *Structure* 4:1153–1159.
18. Polekhina G, *et al.* (1996) Helix unwinding in the effector region of elongation factor EF-Tu–GDP. *Structure* 4:1141–1151.
19. Sengupta J, *et al.* (2008) Visualization of the eEF2–80S ribosome transition-state complex by cryo-electron microscopy. *J Mol Biol* 382:179–187.
20. Zeidler W, *et al.* (1996) Limited proteolysis and amino acid replacements in the effector region of *Thermus thermophilus* elongation factor Tu. *Eur J Biochem* 239:265–271.
21. Munishkin A, Wool IG (1997) The ribosome-in-pieces: Binding of elongation factor EF-G to oligoribonucleotides that mimic the sarcin/ricin and thiostrepton domains of 23S ribosomal RNA. *Proc Natl Acad Sci USA* 94:12280–12284.
22. Nissen P, *et al.* (1995) Crystal structure of the ternary complex of Phe-tRNA^{Phe}, EF-Tu, and a GTP analog. *Science* 270:1464–1472.
23. Knudsen C, Wieden HJ, Rodnina MV (2001) The importance of structural transitions of the switch II region for the functions of elongation factor Tu on the ribosome. *J Biol Chem* 276:22183–22190.
24. Berghuis AM, Lee E, Raw AS, Gilman AG, Sprang SR (1996) Structure of the GDP-P_i complex of Gly203 → Ala $G_{i\alpha1}$: A mimic of the ternary product complex of G_α-catalyzed GTP hydrolysis. *Structure* 4:1277–1290.

25. Kothe U, Wieden HJ, Mohr D, Rodnina MV (2004) Interaction of helix D of elongation factor Tu with helices 4 and 5 of protein L7/12 on the ribosome. *J Mol Biol* 336:1011–1021.
26. Mohr D, Wintermeyer W, Rodnina MV (2002) GTPase activation of elongation factors Tu and G on the ribosome. *Biochemistry* 41:12520–12528.
27. Piepenburg O, *et al.* (2000) Intact aminoacyl-tRNA is required to trigger GTP hydrolysis by elongation factor Tu on the ribosome. *Biochemistry* 39:1734–1738.
28. Saarma U, Remme J, Ehrenberg M, Bilgin N (1997) An A to U transversion at position 1067 of 23S rRNA from *Escherichia coli* impairs EF-Tu and EF-G function. *J Mol Biol* 272:327–335.
29. Li W, Sengupta J, Rath BK, Frank J (2006) Functional conformations of the L11-ribosomal RNA complex revealed by correlative analysis of cryo-EM and molecular dynamics simulations. *RNA* 12:1240–1253.
30. Eargle J, Black AA, Sethi A, Trabuco LG, Luthey-Schulten Z (2008) Dynamics of recognition between tRNA and elongation factor Tu. *J Mol Biol* 377:1382–1405.
31. Grassucci RA, Taylor DJ, Frank J (2007) Preparation of macromolecular complexes for cryo-electron microscopy. *Nat Protoc* 2:3239–3246.
32. Berk V, Zhang W, Pai RD, Cate JHD (2006) Structural basis for mRNA and tRNA positioning on the ribosome. *Proc Natl Acad Sci USA* 103:15830–15834.
33. Schlitter J, Engels M, Krüger P, Jacoby E, Wollmer A (1993) Targeted molecular dynamics simulation of conformational change—Application to the T → R transition in insulin. *Mol Sim* 10:291–308.
34. Humphrey W, Dalke A, Schulten K (1996) VMD—Visual Molecular Dynamics. *J Mol Graphics* 14:33–38.